

Chapter 2

Strategy for Using SVE/BV

2-1. Introduction

This chapter outlines the overall strategy for using SVE/BV and reviews the underlying principles of contaminant transport and removal. The physical and chemical properties of contaminants that influence their fate and movement are identified and introduced, as are the pertinent soil properties. A brief primer on vapor transport through soil is also provided.

2-2. SVE/BV Application Strategy

A phased approach is recommended in applying SVE or BV.

a. If early stages of evaluation indicate that these technologies are not applicable to a site, a change in course can be made before expending unnecessary resources. Figure 2-1 broadly summarizes the process whereby the project team undertakes screening and bench- and pilot-scale testing. Given favorable results, the team then designs the full-scale system, starts it up, performs operations and maintenance, and, at the appropriate time, shuts the system down. Figure 2-1 also presents the primary considerations that enter into each step of the phased approach. It assumes that basic site characterization addressing the nature and extent of contamination and hydrogeological setting has been completed.

b. Applying the appropriate human resources is an essential component of the SVE/BV strategy. Depending on the particular phase of the project being confronted, and on site-specific conditions and objectives, a variety of staff specialists may need to be involved. These will likely include one or more engineers, geologists, hydrogeologists, soil scientists, and chemists. Even in a relatively small project, assembling a project team appropriate for the problem is essential. Not all team members would work extensively on the project, rather they may just consult on specific issues, but their input may be very important to achieving success. A diverse team is best able to identify the information needed to make decisions as early as possible. EM 200-1-2 provides additional guidance regarding project planning.

2-3. Fundamental Principles

The factors that determine vapor phase contaminant fate and transport in the unsaturated zone are summarized below. Contaminant transport and removal, contaminant characteristics, porous medium characteristics, and principles of vapor flow are described. See USEPA 1991b for a more complete discussion of this material.

a. Contaminant transport and removal. The removal of VOCs and SVOCs by SVE/BV can be controlled by a number of processes. Transport and removal mechanisms include advection, volatilization, desorption, biodegradation, and diffusion. Figure 2-2 illustrates the processes that occur in soil contaminated by VOCs and the mechanisms of contaminant removal (USEPA 1991c). In the hypothetical example illustrated, VOCs exist in the vadose zone as residual nonaqueous phase liquid (NAPL) retained by capillary forces between solid particles; as adsorbed organics associated with solid surfaces; as dissolved

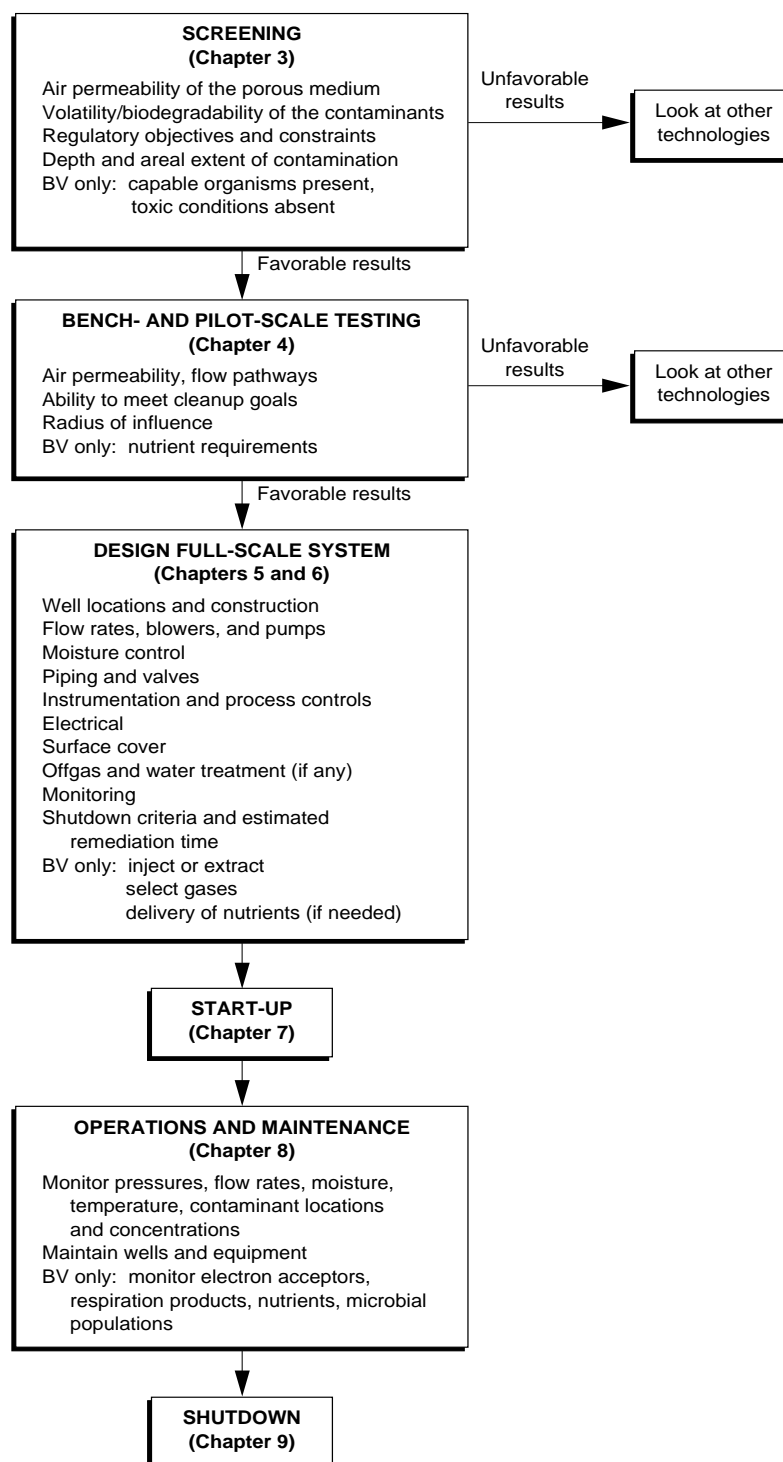


Figure 2-1 SVE/BV Application Strategy

organics in soil pore water; and as free organic vapor in the soil pore gas. The distribution of VOCs among liquid, solid, and gaseous phases is governed by various physical phenomena as described in paragraph 2-3*b*. Figure 2-2 also depicts light NAPL (LNAPL) within the capillary fringe and pooled on the water table, as well as pools of dense NAPL (DNAPL) pooled below the water table within depressions in the bedrock surface. Where both LNAPL and DNAPL compounds are present at the same site, co-solvation of one within the other may occur.

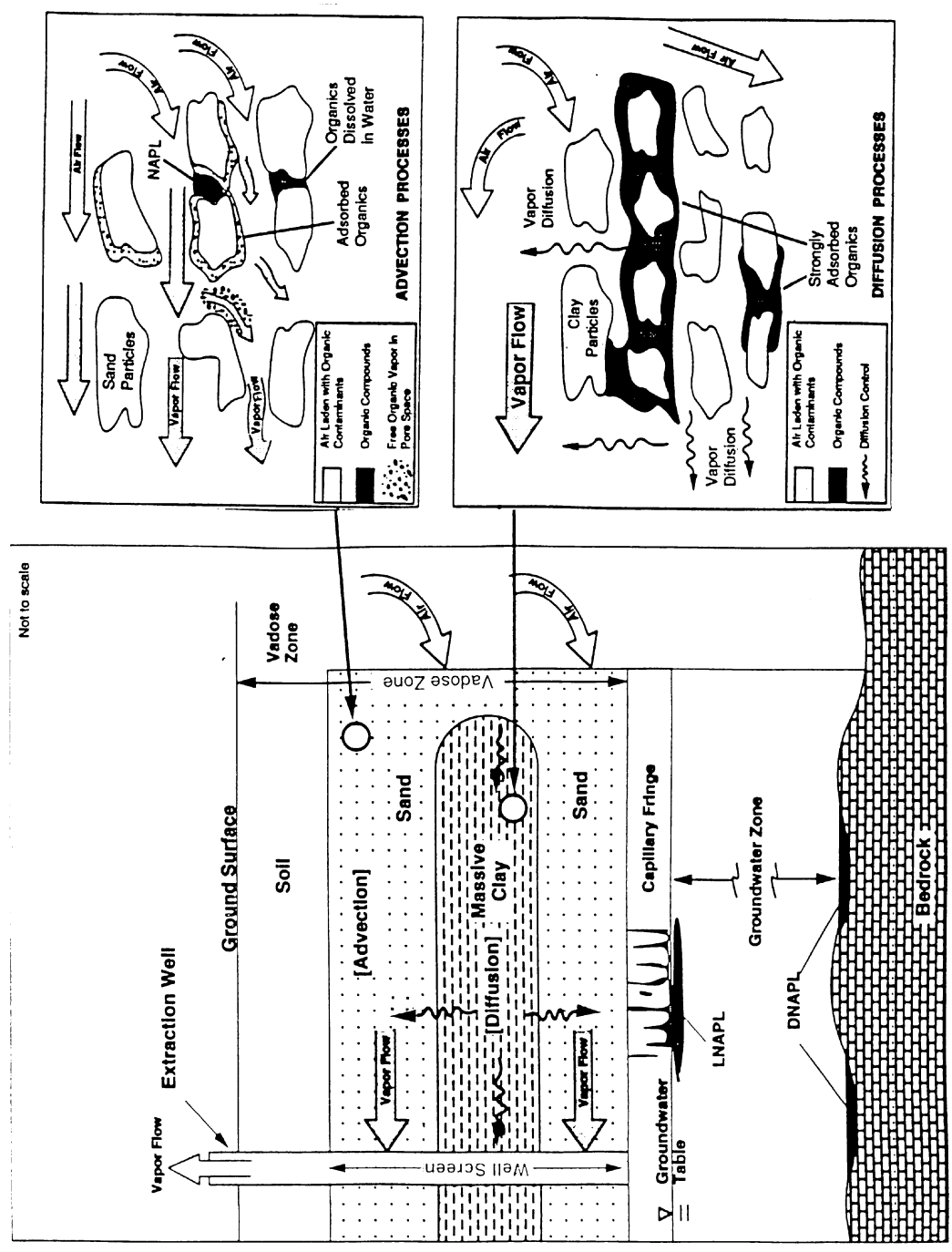
(1) As air is drawn through the soil during SVE/BV, contaminants that volatilize into the vapor phase are carried along with the bulk movement of the air through more permeable regions in a process known as advection. Advection through low permeability regions is relatively slow. However, where concentration gradients exist between pores being swept by the flowing air and contaminated soil not in communication with the airstream, contaminants will move by diffusion toward the flowing air. Generally, diffusion is much slower than advection and will limit the rate of contaminant removal from less permeable zones.

(2) Fastest removal rates theoretically would occur in cases where contaminants are fully volatilized and reside in interconnected soil pores. In such a situation, removal would be limited by the advection rate, and the removal rate could be increased simply by increasing the airflow rate. This is hardly ever the case, however, and other factors usually limit contaminant removal rates. The rate of volatilization of contaminants from a NAPL or an aqueous phase is often limiting. Desorption of contaminants from soil particle surfaces can also be the limiting process (Novak, Young, and Forsling 1993). Nonequilibrium effects are further discussed in paragraph 2-3*b*, and their manifestations are presented in paragraph 9-9. The following paragraphs underscore the importance of recognizing and designing for nonequilibrium conditions.

(3) Johnson, Palmer, and Keely (1987) studied the effect of soil moisture on the diffusion of VOCs in soil columns. Travel times were two to three times longer in damp sand than in dry sand. The delay was attributed to the effect of partitioning to the pore water. Many sites with LNAPL such as gasoline or fuel oil will have a zone of residual contamination in the vicinity of the water table and capillary fringe. Diffusion of contaminants to the overlying unsaturated zone is often the limiting transport mechanism at such sites.

(4) On a larger scale, contaminant removal at a site will generally commence in more permeable zones and proceed to progressively less permeable zones. Soil stratigraphy will in this sense limit contaminant removal. Clay lenses containing NAPL, for example, can serve as continuing sources of vapor phase contaminants long after adjacent, more permeable zones have been remediated. Stratigraphy is extremely important to consider in designing the remediation system and projecting completion times.

(5) There is a risk to "overdesign" SVE systems, using higher venting flow rates than necessary (Payne 1993). In many cases, higher flow rates do not improve removal but do increase offgas treatment costs. To design SVE and BV systems as economically as possible, venting flow rates should be minimized in order to reduce offgas volumes and maximize contaminant concentrations in the offgas, thereby maximizing contaminant removal per unit cost of moving air. This should be carefully weighed against the competing need to provide adequate air flow between air extraction and injection points to find an optimal operating point. To achieve adequate air flow between wells, it is often necessary to induce large air flows near the extraction or injection wells. It is desirable to identify the removal rate-limiting step at a site and determine the minimum venting flow rates which will effectively remediate the site, as discussed further in Chapters 5 and 9.



Source: after USEPA 1991c

Figure 2-2 SVE Transport Processes

3 Jun 02

b. Contaminant properties. Physical and chemical properties strongly influence the fate and transport of contaminants. These properties affect the distribution of the contaminants among the four phases in which they can exist in soil, namely as vapor (gaseous phase), dissolved in pore water (aqueous phase), adsorbed on the surface of particles (solid phase), and as NAPL (Figure 2-3). The degree to which a compound partitions into the vapor phase, at equilibrium, is indicated by the compound's vapor pressure, Henry's law constant, and boiling point. The degree to which a compound, at equilibrium, will dissolve in water is described by the compound's solubility. Finally, the degree to which a compound, at equilibrium, will adsorb to soil is indicated by the soil adsorption coefficient. In a mixture of contaminants (such as a petroleum product) the distribution of compounds among the four phases will change as weathering occurs over time after its release into the environment. Early on, the lighter, more volatile, and more soluble fractions tend preferentially to be subject to various removal mechanisms. The heavier, less soluble, and less volatile fractions, meanwhile, have a greater tendency to persist in association with the soil matrix. Appendix B provides a compendium of tables listing contaminant properties.

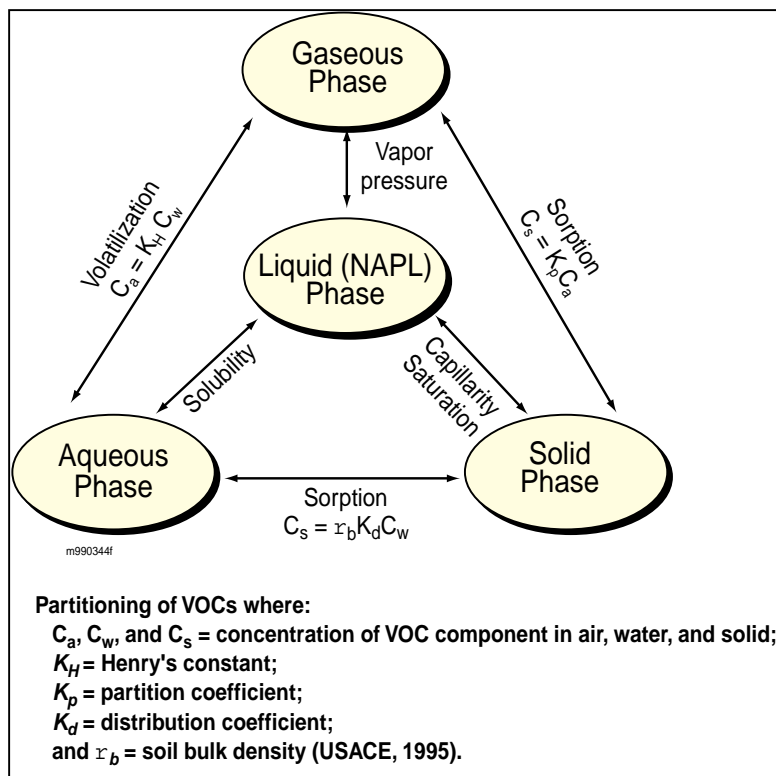


Figure 2-3 Partitioning of VOCs

(1) Vapor pressure is the tendency of a solid or liquid to evaporate, or more specifically, the force per unit area exerted by the vapor of the chemical in equilibrium with its solid or liquid form. For example, gasoline placed in a sealed container will evaporate and diffuse throughout the headspace until an equilibrium is reached. The gasoline vapor in the headspace exerts a pressure on the container. The pressure within the headspace can be measured, usually as millimeters of mercury (mm Hg) or inches of water, in a manometer connected to the headspace. Vapor pressure increases strongly with increasing temperature. Vapor pressure is applicable when NAPL is present. Vapor pressure P_v (Pa) can be converted to vapor density or concentration C_v (g m^{-3}) with the Ideal Gas Law

$$C_v = M P_v / R T \quad (2-1)$$

with molecular weight M (g mol^{-1}), universal gas constant R ($8.314 \text{ Pa m}^3 \text{ mol}^{-1} \text{ K}^{-1}$), and temperature T (K).

(2) Raoult's law provides an approximation of the vapor pressures of compounds over a NAPL mixture such as a petroleum product. Raoult's law states that the partial vapor pressure P_{vi} of a constituent i in a gaseous mixture is equal to the mole fraction X_i of constituent i in the NAPL, times the vapor pressure P_i° of the pure constituent i (which is a function of temperature):

$$P_{vi} = X_i P_i^\circ \quad (2-2)$$

(3) Henry's law determines the extent of volatilization of a contaminant dissolved in water. The Henry's constant K_H expresses the ratio of the compound's concentration in the vapor phase C_v (mass/volume air) to the compound's concentration in the liquid phase C_l (mass/ volume of liquid), at equilibrium

$$K_H = C_v/C_l \quad (2-3)$$

The ratio is therefore defined as mass per unit of vapor divided by mass per unit of liquid, or equivalently, mole fraction in the vapor phase divided by mole fraction in the liquid phase. In either case, Henry's law constant is not truly dimensionless. Care must be exercised with Henry's constants because they can be given as K_H above, or as k_H in units such as atm-ml/gram or, more commonly, atm-m³/mole. The Henry's constant for a given compound increases strongly with increasing temperature.

(4) Boiling point indicates the temperature at which a compound's vapor pressure equals the vapor pressure of the atmosphere, which at sea level is approximately 760 mm Hg. Atmospheric pressure, and thus boiling point, decreases significantly with increasing elevation above sea level. Inducing a vacuum in soil causes the pressure in the air-filled soil pores to decrease, leading in turn to a lowering of the boiling point and an increase in volatilization of the contaminant.

(5) Soil distribution coefficient (K_d) indicates the tendency of a compound in solution to adsorb to the surface of particles of soil or organic matter. At equilibrium, a nonpolar organic compound is thus seen to distribute itself between solution concentration C_w and sorbed concentration C_s , as a function of their ratio: $K_d = C_s/C_w$, with K_d being equal to the soil sorption or partition coefficient. The value of K_d for a given organic compound is not constant, however, but tends to increase linearly for soils with increasing organic carbon (OC) and clay contents. The slope of the relationship between K_d and % organic C is the amount of sorption on a unit carbon content basis (K_{oc}) (Hassett and Banwart 1989) in which $K_{oc} = K_d/f_{oc}$ (where f_{oc} is the fraction of organic content in the soil). Thus K_{oc} values may be viewed as sorption coefficients normalized to organic carbon content.

(6) K_{oc} values are not often readily available, and octanol-water partition coefficients (K_{ow}), which are highly correlated with K_{oc} values, are commonly used as indicators of the tendency for adsorption. K_{ow} is the equilibrium ratio of the contaminant concentration in *n*-octanol to the contaminant concentration in distilled water. There are numerous equations that have been empirically developed relating K_{ow} to K_{oc} (Dragun 1988). If the K_{ow} of a constituent of concern is known, its K_{oc} can be calculated and then its soil adsorption coefficient (K_d) can be estimated by multiplying the K_{oc} by the f_{oc} .

(7) Although soil adsorption coefficients imply equilibrium and reversible sorption, soil/fluid/vapor partitioning processes are often neither in equilibrium nor reversible and are, therefore, not well predicted by soil adsorption coefficients. Two-compartment sorption models are hypothesized to explain this behavior wherein sorbed compounds may not desorb as readily as predicted because, over time, they can become more strongly associated within less accessible sorption sites or more resistant soil fractions. Release of compounds from dead-end micropores is similarly recognized to be diffusion-limited (Scow, Simkins, and Alexander 1986; Pignatello 1989). Thus, compounds may not be as susceptible to volatilization or leaching or as bioavailable as would be expected if their fate was not desorption limited. As a consequence, compounds can prove to be more persistent during treatment than would otherwise be expected.

(8) Solubility determines the degree to which a contaminant dissolves into groundwater and unsaturated zone pore water. Compounds with high solubility are usually more mobile in infiltrating precipitation and groundwater and are also generally more biodegradable than less soluble compounds.

(9) The biodegradability of contaminants vary substantially even among compounds of the same class, such as petroleum hydrocarbon. Factors such as solubility, temperature, oxygen availability, pH, and presence of toxicants affect the biodegradation kinetics of contaminants. Biodegradation kinetics may significantly affect the rate of site remediation by SVE/BV.

c. Soil properties. Like contaminant physical and chemical properties, porous medium and fluid characteristics strongly influence contaminant fate and transport.

(1) Texture describes the size range of particles in the soil. A textural characterization can be either qualitative, as when a soil is broadly referred to as sandy or clayey, or quantitative, as when the distribution of particle sizes is measured by a mechanical analysis. In the latter case, textural classifications can be applied using standardized systems (e.g., U.S. Department of Agriculture (USDA) system; ASTM Unified Soil Classification System). The distribution of pore sizes in the subsurface is ultimately more important to considerations of SVE/BV than is the distribution of particle sizes, because it is through the pores that fluid flow occurs. A relationship exists between pore size and particle size with coarser grained soils generally having larger pore spaces and fine-grained soils generally having smaller pore sizes.

(1) Porosity (n) is the (dimensionless) ratio of the void volume (V_v) to the total volume (V_t) of the porous medium, usually expressed as a decimal fraction or percent. Soil pores can be occupied by vapor, water, and/or NAPL. Porosity can be calculated from the bulk density of the soil (ρ_b) which is the dry weight of soil per bulk volume (i.e., of both soil and pore space) by

$$n = 1 - (\rho_b / \rho_s) \quad (2-4)$$

with particle density ρ_s . For many inorganic soil particles, ρ_s is approximately equal to 2.65 g/cm^3 . Air-filled porosity is designated n_a . Geotechnical engineers typically term ρ_b the dry density.

(1) Saturation (S) is the volume of a fluid per volume of soil pore space V_{pores} . When expressed as a percentage, it is termed “degree of water saturation”, S_w (dimensionless), i.e. $S_w = V_w / V_{\text{pores}}$. Moisture content, by contrast, is the amount, by weight or volume, of liquid water in a soil. When expressed on a mass basis, moisture content w is the mass of water (M_w) in a soil sample divided by its oven-dry mass (M_{soil}), $w = M_w / M_{\text{soil}}$. When expressed on a volume basis, moisture content θ is the volume of water (V_w) in a sample divided by the total bulk volume (V_t) of the sample, $\theta = V_w / V_t$. Thus, $S_w = \theta / n$. To obtain volumetric moisture content from gravimetric moisture content, use the relation $\theta = w \rho_b / \rho_w$, where ρ_w is the density of water. Moisture content reduces the air-filled porosity of a soil and the number of air pathways. Air permeability is greater at lower moisture contents because a larger percentage of the pore space is available for vapor transport. In SVE, however, it is desirable to have some moisture content in the soil because desorption of contaminants from soil increases if films of water are present to displace contaminant molecules (USEPA 1991d). BV systems require at least 50 percent field capacity (preferably 75 to 80 percent of field capacity) to function optimally. Field capacity can be determined by saturating undisturbed soil samples, allowing the free water to drain and then measuring the moisture content. Field capacity is

the mass of water in the sample divided by the dry weight after allowing a saturated soil to drain for 24 hours. Because field capacity is a frequently misunderstood term, discussions of the concept and methods of measurement/prediction should be consulted (Hillel 1980b; Cassel and Nielsen 1986). Table 4-8 of this document provides some typical field capacity values for 12 types of soil.

(4) Wetting and nonwetting phases. In a porous medium containing two fluid phases (e.g., water and air), the wetting phase is the fluid that occupies positions closest to points of contact between solid phase particles, while the nonwetting phase is the fluid that occupies positions more removed from interparticle contact points. For the case in which the soil pores are occupied either by water or air, water is usually considered the wetting phase and air the nonwetting phase. The nonwetting (i.e., air) phase saturation S_{nwa} is then defined as $1 - S_w$, where S_w is the degree of water saturation. When another nonwetting phase such as oil is also present, it is considered nonwetting with respect to water and wetting with respect to air, and its saturation S_{now} can be defined such that $S_w + S_{nwa} + S_{now} = 1$.

(5) Residual water saturation S_r is the volume fraction of immobile water. Such water occupies disconnected pores and cannot flow because it is held in place by capillary forces. Capillary forces are intrinsically greater in finer-grained soils, due to the smaller pore (or capillary) sizes. Accordingly, the residual water saturation in clay and silt layers will tend to be higher than in adjacent sand and gravel layers. This tends to accentuate the lithologic influence on air permeability.

(6) Residual NAPL saturation S_{ro} is the degree of NAPL saturation which remains in a soil that, having contained NAPL, is subjected to drainage until the NAPL- filled pore spaces are discontinuous. Residual NAPL saturation varies with soil type, NAPL type, and moisture content. Ganglia are isolated globules of NAPL that may collect in subsurface pools, cracks, or fissures.

(7) Capillary pressure P_c between two phases (e.g., air and water or oil and water) is defined as

$$P_c = P_n - P_w \quad (2-5)$$

where P_n and P_w are the nonwetting and wetting phase pressures [$ML^{-1}T^{-2}$], respectively (N.B: the use of square brackets indicates dimensions, with M = mass; L = length; and T = time.). Capillary pressure can be expressed in terms of pressure head h_c , (also known as capillary pressure head or simply capillary head) by observing that under hydrostatic conditions, $h = P/\rho g$, with h = pressure head [L]; ρ = density [$M L^{-3}$]; and g = acceleration of gravity [$L T^{-2}$]. Thus, dividing Equation 2-5 through by ρ and g ,

$$h_c = h_n - h_w \quad (2-6)$$

where h_n and h_w are the nonwetting and wetting phase pressure heads, respectively. In unsaturated porous media, capillary pressures are less than atmospheric pressure. Since a liquid in equilibrium with atmospheric pressure is, by convention, assigned a pressure head value of zero, unsaturated soils that contain air-filled pores connected to the atmosphere have liquid-phase pressure heads that are less than zero, i.e., negative. In air-water systems, such negative heads are often expressed as positive values of capillary pressure head (also known as tension head, matric suction, or simply suction, ψ) (Hillel 1980a), i.e., $h_c = -\psi$. By contrast, pressures are sometimes expressed in terms of absolute pressure relative to a reference pressure of zero in an absolute vacuum. Table 2-1 summarizes typical conversions among various units of pressure and pressure head.

Table 2-1 Pressure/Pressure Head Conversions

Units of Pressure	
1 bar=	10^5 N m^{-2}
=	0.987 atmospheres
=	14.5 psi
=	$10^6 \text{ dynes cm}^{-2}$
=	100 kPa

Units of Pressure Head	
and is equivalent to:	1033 cm column of water
	75.99 cm column of Hg

Example:

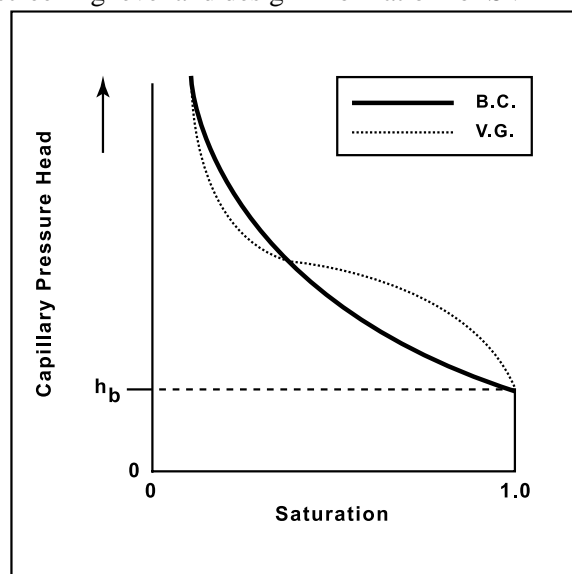
A vacuum gauge mounted on the wellhead of a vent well reads in cm H₂O (gauge). In other words, it reads 0 cm H₂O when the air in the well is at atmospheric pressure. When a blower is turned on and exerts a vacuum on the well, the gauge reads a vacuum head of 100 cm H₂O, which is equivalent to a vacuum head of 7.35 cm Hg.

$$\text{i.e., } \frac{100 \text{ cm H}_2\text{O}}{1020 \text{ cm H}_2\text{O}} = \frac{7.35 \text{ cm Hg}}{75.01 \text{ cm Hg}} = \frac{9.8 \text{ kPa}}{100 \text{ kPa}}$$

These can also be expressed as gauge pressure heads of -100 cm H₂O or -7.35 cm Hg, or as a gauge pressure of -9.8 kPa.

The readings can, if desired, be converted to absolute pressures/pressure heads, as follows: Atmospheric pressure plus gauge pressure equals absolute pressure. Therefore, if barometric pressure = 101.32 kPa, absolute pressure = 101.32 kPa + (-9.8 kPa) = 91.52 kPa. An equivalent absolute pressure head is 76.0 cm Hg + (-7.35 cm Hg) = 68.65 cm Hg.

(8) Capillary pressure head-saturation curves (also known as moisture retention curves, soil moisture characteristic curves, or $h_c(S)$ curves) can provide useful screening level and design information for SVE and BV. Not only do such curves reflect the pore-size distribution of the soil, they also reveal the energy associated with soil water at various levels of saturation (Figure 2-4). As water saturation declines, the remaining water is held more and more tenaciously within smaller and smaller soil pores, and increasingly more energy per unit weight of water (i.e., head) is required to extract it. Upon the imposition of a vacuum on an SVE well in a formation that includes lenses of soil or zones that are initially saturated, the largest pores empty of water first, at the *air entry suction* (also known as the *bubbling pressure head*, h_b), followed by incrementally smaller pores as smaller values of capillary pressure head (i.e., larger suctions) are applied by the vacuum. The onset of air permeability in an initially saturated porous medium, corresponding to the air entry value, occurs when the gaseous phase first occupies an interconnected network of air-filled pores. This air entry value,



M010072

Figure 2-4 Capillary pressure head-saturation curves exhibiting Brooks-Corey (B.C.) and Van Genuchten (V.G.) Analytical Functions

which can be inferred from a capillary pressure head-saturation curve, gives an indication of the vacuums that will need to be exerted on a wet soil to implement SVE/BV. The “B.C.” curve illustrated in Figure 2-4 has the shape of a Brooks-Corey analytical function, (Brooks and Corey 1966), and is most appropriate to represent soils exhibiting sharp air entry suctions. Soils that do not exhibit such behavior may be better represented by a Van Genuchten (1980) analytical function, as depicted by the “V.G.” curve in Figure 2-4.

(9) Permeability or intrinsic permeability (k) is a measure of the ease with which a porous medium can transmit air, water, or other fluid. Intrinsic permeability is a function only of the porous medium and has dimensions of length squared [L^2]. Permeability may also be expressed in units of darcies: 1 cm^2 is approximately equivalent to 10^8 darcies. When permeability is expressed as a fraction of the maximum permeability value that the medium can exhibit for a given fluid, it is termed *relative permeability*, k_r (dimensionless).

(10) Hydraulic conductivity (K) is a measure of the ease with which a porous medium can transmit a specific fluid, usually water. Hydraulic conductivity is a function of both the porous medium and the fluid, and has dimensions [$L T^{-1}$]. When hydraulic conductivity is determined under water-saturated conditions, it is known as the saturated hydraulic conductivity (K_s). Intrinsic permeability is related to saturated hydraulic conductivity as follows:

$$k = K_s \mu_w / \rho_w g \quad (2-7)$$

where μ_w is the dynamic viscosity of water [$M L^{-1} T^{-1}$] and ρ_w is the density of water [$M L^{-3}$]. For water at approximately 293 K, $k = (10^{-7} \text{ m-sec})(K_s)$, where k is expressed in units of m^2 and K_s in mAsec^{-1} , or $k = (10^{-5} \text{ cm-sec})(K_s)$ where k is expressed in units of cm^2 and K_s in cm sec^{-1} .

(11) Air permeability (k_a) is the ability of vapors to flow through the porous medium. It is a property of the porous medium only and has dimensions [L^2]. Relative air permeability k_{ra} expresses air permeability as a (dimensionless) fraction of intrinsic permeability, $k_{ra} = k_a/k$. Air permeability is perhaps the most important soil parameter with respect to the success and design of SVE/BV systems. Air prefers to flow through zones of higher air permeability (i.e., paths of least resistance), and the air permeability of the subsurface should be well characterized before implementing SVE or BV. Because air-filled porosity determines the pore volume available for vapor transport, air permeability is a function of saturation. As the degree of water saturation decreases, and as air-filled porosity increases accordingly, the relative permeability of the soil to air increases as a steeply nonlinear function of the degree of saturation.

(a) Models are available for predicting the dependence of relative permeability on saturation, given measured capillary pressure head-saturation data for a soil. Brooks and Corey (1966) developed analytic functions relating capillary pressure head to saturation that can be fit to measured $h(S)$ data, and used to predict the dependence of relative air permeability on saturation, $k_{ra}(S)$, which is essential for modeling airflow under partially saturated conditions.

(b) The air permeability is significantly influenced by the density and viscosity of the soil gas, both of which are, in turn, a function of temperature. Over the range of temperatures commonly encountered in SVE/BV (280K-295K), density and viscosity will not be affected significantly by changes in temperature. With thermal enhancements, however, such changes can become considerable.

(12) Peclet number is a dimensionless number that relates the effectiveness of mass transfer by advection to the effectiveness of mass transfer by diffusion. Peclet numbers have the general form of vd/D where v is the velocity, d is the characteristic length scale, which in this case is the average grain size, and D is the diffusion coefficient of the contaminant in air. For mass transfer parallel to the direction of advective flow, diffusion is dominant at Peclet numbers less than 0.02, and advection is dominant at Peclet numbers greater than 6. For mass transfer perpendicular to advective flow, diffusion dominates at Peclet numbers less than 1, and advection dominates at Peclet numbers greater than 100 (Gillham and Cherry 1982).

(13) Humidity is important in SVE and BV. Water vapor, like liquid water, promotes desorption of contaminants from soil particles. As relative humidity approaches 100 percent, however, liquid water will condense in cooler system components and can, for example, reduce the efficiency of offgas treatment.

2-4. Fundamentals of Vapor Flow in Porous Media

Sites can be modeled to approximate the performance of a SVE/BV system, and to explore design alternatives. Models, however, have to make some simplifying assumptions to represent the site mathematically. In many cases these simplifying assumptions do not affect the final result, but the possibility that they could should be kept in mind. Some of these assumptions may include homogeneous, isotropic conditions, while sites are frequently heterogeneous (e.g., layered) and directionally dependent in their properties. In addition, models are always dependent on the representativeness of the data to the actual site conditions. These considerations are key to understanding the extent to which the model can be expected to accurately predict site performance.

a. Darcy's law for vapor flow. Laminar flow in porous media is generally described by Darcy's law, an empirical relationship of the form

$$q = \frac{k_i \rho g}{\mu} \nabla H \quad (2-8)$$

where

q = discharge per unit area [L/T]

k_i = intrinsic permeability [L^2]

ρ = fluid density [M/L^3]

g = acceleration of gravity [L/T^2]

μ = dynamic fluid viscosity [$M/L-T$]

∇ = gradient operator [L^{-1}]

H = total head [L]*

*Note that a value for pressure can be obtained by multiplying head by ρg .

(1) As described in paragraph 2-3c(9), intrinsic permeability k is a property of the porous medium. Density ρ and viscosity μ are properties of the particular fluid under consideration. Values of viscosity of air at normal temperature and pressure (NTP) are 1.83×10^{-5} newton·s m⁻². This is equivalent to 1.83×10^{-4} gm cm⁻¹ s⁻¹ and 1.83×10^{-2} centipoise. Likewise, values of density of air at NTP are 1.20×10^{-3} Mgm m⁻³, equivalent to 1.20×10^{-3} gm cm⁻³ and 7.49×10^{-2} lb ft⁻³. NTP is a gas industry reference, with normal temperature defined as 21.1 °C (70 °F) and normal pressure as 1 atmosphere (101.35 KPa or 14.6960 psia).

(2) Head H (energy per unit weight) [L] can be expressed equivalently as pressure P (energy per unit volume) [ML⁻¹T⁻²] and as potential ϕ (energy per unit mass) [L²T⁻²]. To convert head to pressure, multiply head by ρg , where ρ is the density of the fluid and g the acceleration of gravity. To convert head to potential, multiply head by g . Finally, to convert pressure to potential, divide pressure by ρ (Hillel 1980a).

(3) Total fluid potential ϕ (i.e., mechanical energy per unit mass) [L²T⁻²] is defined by Bernoulli's equation:

$$\phi = gz + \frac{v^2}{2} + \int_{P_o}^P \frac{1}{\rho} dP \quad (2-9)$$

where

z = elevation [L]

v = fluid velocity [L/T]

P = absolute pressure [M/LT²]

(a) The first term of Equation 2-9 is gravitational potential, the second term is inertial potential, and the third term is pressure potential. For vapor flow, gravitational effects are small for the elevation differences under consideration. Likewise, inertial effects can be neglected for laminar flow. As a result, the gradient of total fluid potential ϕ becomes

$$\nabla \phi = \frac{1}{\rho} \nabla P \quad (2-10)$$

and Darcy's law for vapor flow is

$$q = \frac{k_a}{\mu} \nabla P \quad (2-11)$$

(b) Note that intrinsic permeability k_i has been replaced by air permeability k_a in Equation 2-11. Whereas intrinsic permeability is a measure of the resistance to flow through the total pore space, air permeability represents the resistance to flow through only the air-filled pore space. Since the air-filled porosity deviates from the total porosity by the amount of water saturation, air permeability generally is lower than intrinsic permeability (paragraph 2-3c).

(4) Klinkenberg (1941) showed that for clayey materials, gas slippage occurs, resulting in higher flow rates than those predicted by Darcy's law. Gas slippage, commonly referred to as the Klinkenberg effect, results from nonzero flow velocities along pore walls. Massmann (1989) indicates that, for pore radii greater than approximately 10^{-3} mm, the effects of slip flow are small relative to viscous flow and can be neglected. As described below, McWhorter (1990) has developed an exact solution for radial flow incorporating gas slippage.

b. Partial differential equation for vapor flow. The partial differential equation for vapor flow is developed by combining Darcy's law with the principle of conservation of mass. Conservation of mass, for a compressible fluid, states that

$$\nabla \bullet (\rho q) = \frac{\partial (\rho n_a)}{\partial t} \quad (2-12)$$

where

n_a = air-filled porosity

Substituting Darcy's law into Equation 2-12 yields:

$$\nabla \bullet \left(\rho \frac{k_a}{\mu} \nabla P \right) = \frac{\partial (\rho n_a)}{\partial t} \quad (2-13)$$

Expressing vapor density in terms of pressure using the ideal gas law (Equation 2-1), and treating porosity and viscosity as constants, Equation 2-13 reduces to

$$\nabla \bullet (k_a \nabla P^2) = 2 n_a \mu \frac{\partial P}{\partial t} \quad (2-14)$$

(1) This is a nonlinear partial differential equation with few exact solutions. The primary source of nonlinearity in SVE/BV applications is the dependence of gas density upon pressure (McWhorter 1990). Other sources of nonlinearity include pressure-dependent viscosity, gas slippage, and nonlaminar flow. Nonlaminar flow occurs under high pressure gradients (such as in petroleum reservoirs), whereas gas slippage typically occurs only in clayey soils.

c. Steady state vapor flow.

(1) Since most SVE/BV systems are designed for long-term operation, steady-state flow models are appropriate for system design. Steady-state solutions can be used for air permeability tests, provided that

sufficient time is allowed for flow to stabilize. For the case of one-dimensional radial flow, steady-state solutions can also be used to analyze transient permeability test data, for a condition known as the pseudo-steady state (paragraph 2-4e). This method incorporates pressure-dependent density, which is not possible using the more common transient analysis methods (e.g., Johnson, Kemblowski, and Colthart (1990b)).

(2) The partial differential equation for steady-state flow is obtained by setting the right-hand side of Equation 2-14 equal to zero

$$\nabla \bullet (k_a \nabla P^2) = 0 \quad (2-15)$$

(3) For isotropic conditions, k_a is independent of $\nabla^2 P^2$, and

$$\nabla^2 P^2 = 0 \quad (2-16)$$

(4) Equation 2-16 is equivalent to Laplace's equation in P^2 . Laplace's equation is a classical partial differential equation that is used to solve problems involving potential flow. Functions that satisfy Laplace's equation include both stream functions and potential functions.

(5) Equation 2-16 can be solved using analytical or numerical methods. Analytical methods involve finding closed-form integrals that satisfy Equation 2-16. Numerical methods involve discretizing the flow domain into a grid, and solving Equation 2-16 using iterative techniques. Numerical methods can be used to evaluate heterogeneous systems with irregular geometries, whereas analytical methods are better suited for homogeneous systems with idealized geometries. However, permeability tests are most commonly analyzed using analytical solutions. Since these solutions illustrate the general principles of flow, the following development is based on analytical methods.

(6) For linear flow in the one dimension, Equation 2-16 is

$$\frac{d^2 P^2}{dx^2} = 0 \quad (2-17)$$

where

x = the one-dimensional cartesian coordinate [L]

For horizontal flow to a long, fully penetrating trench, with $P = P_{atm}$ at $x = L$, the solution to Equation 2-17 is:

$$P^2 - P_{atm}^2 = \frac{2 Q_L P^* \mu}{b k_a} (L - x) \quad (2-18)$$

where

Q_l = volumetric flow rate per unit length of trench [L^2/T]

P^* = absolute pressure at the point of flow measurement [M/LT^2]

b = thickness of the vadose zone [L]

This equation can be used to calculate the lateral pressure distribution near a long trench, for a vadose zone with upper and lower impermeable boundaries. Alternatively, it can be used to determine the required spacing between alternating extraction and passive inlet trenches, where L is the distance between trenches.

(7) For radial flow in one dimension, Equation 2-16 is

$$\frac{d^2 P^2}{dr^2} + \frac{1}{r} \frac{d P^2}{dr} = 0 \quad (2-19)$$

where

r = the one-dimensional radial coordinate (equivalent to $[x^2 + y^2]^{1/2}$ in cartesian coordinates)

The solution to this equation for horizontal flow to a line sink at $r = 0$, with $P = P_i$ at $r = r_i$ is

$$P^2 - P_i^2 = \frac{Q_v P^* \mu}{\pi b k_a} \ln\left(\frac{r_i}{r}\right) \quad (2-20a)$$

or, if $Q_v > 0$ (i.e., if the extraction flow rate is considered positive)

$$P^2 - P_i^2 = \frac{Q_v P^* \mu}{\pi b k_a} \ln\left(\frac{r}{r_i}\right) \quad (2-20b)$$

where

Q_v = volumetric flow rate [L^3/T]

(8) Equation 2-20 can be used to estimate k_a based on field measurements at a tightly covered or highly anisotropic (vertical permeability much smaller than horizontal permeability) site, such as during a pilot test, by measuring P_i while extracting at constant Q_v . If k_a is known at a tightly covered or anisotropic site, then equation 2-20 can be used to estimate the pressure distribution surrounding an extraction well at steady state.

(9) By extrapolating equation 2-20 to the radius at which $P = P_{atm}$, the radius of pressure influence (r_e) can be determined. In a practical sense, r_e is the limit of measurable pressure influence resulting from an extraction well. The radius of pressure influence may be obtained by fitting data from multiple observation

points to Equation 2-20, or it can be obtained by preparing a semilog plot of pressure versus distance (Figure 2-5). This type of plot often termed a distance-drawdown graph (Driscoll 1986).

(10) However, the radius of pressure influence, r_e , is both somewhat problematic, and misunderstood.

(a) Mass balance dictates that for continuous withdrawal of air from a stratum with impermeable upper and lower boundaries, r_e must increase with time. This conclusion is borne out by analyses of transient

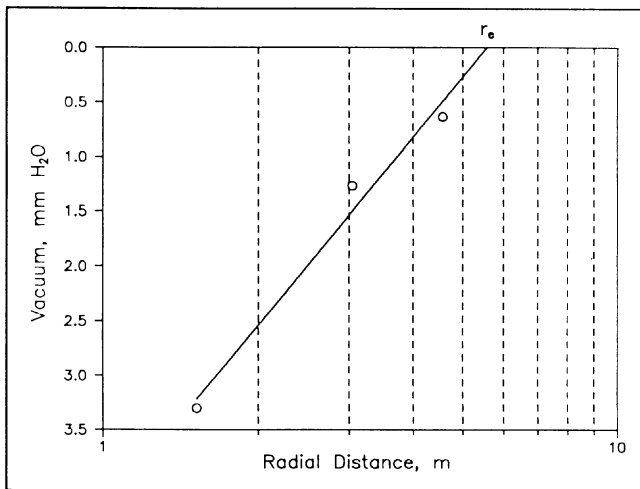


Figure 2-5 Use of distance-drawdown graphs to determine r_e

radial flow, which indicate that r_e increases in proportion to the square root of time (McWhorter and Sunada 1977; McWhorter 1990). However, the widespread acceptance of a fixed r_e reflects the common field observation that the limit of radial pressure influence often shows little change over time. This phenomenon may be explained by leakage of air through upper and lower boundaries, attesting to the rarity of truly horizontal flow. As mentioned above, the widespread observation that r_e often shows little change over time attests to the rarity of one-dimensional radial flow. Beckett and Huntley (1994) conclude that even where the ground surface is paved, vertical leakage is the rule, rather than the exception. Vertical leakage results in

two-dimensional radial flow.

Historically, r_e has been used as the basis of design for extraction well networks. Designers have interpreted the zone of vacuum influence around a well as also corresponding to the “capture zone” of the extraction well. By subsequently selecting an arbitrary distance within this zone of vacuum influence (e.g., the radius at which the vacuum equals 0.25 cm water vacuum), designers have established well spacings for SVE well networks. Unfortunately, this is a completely inappropriate interpretation of this phenomenon. As described further in Chapter 5, SVE designs should be based on pore gas velocities or the rates of pore gas exchange, which, are a function of both the pressure (vacuum) distribution around the extraction point and the associated soil air permeability. Thus, using Figure 2-5 directly for SVE design purposes is not appropriate.

(11) An analytical solution for two-dimensional flow to a well can be obtained by superposition of a point sink solution along the length of the well screen. Equation 2-16 for two-dimensional radial flow is:

$$\frac{\partial^2 P^2}{\partial r^2} + \frac{1}{r} \frac{\partial P^2}{\partial r} + \frac{\partial^2 P^2}{\partial z^2} = 0 \quad (2-21)$$

where

r = the horizontal radial coordinate (equivalent to $[x^2 + y^2]^{1/2}$ in cartesian coordinates)

z = the vertical radial coordinate (equivalent to the vertical cartesian coordinate)

The solution to this equation for a point sink located at $r = 0$, $z = z'$ in an infinite space, is

$$P^2 - P_{atm}^2 = \frac{Q_v P^* \mu}{2 \pi k_a} \frac{l}{\sqrt{r^2 + (z - z')^2}} \quad (2-22)$$

where

z' = z -coordinate of the point sink

The point sink solution can be integrated with respect to z to obtain a line sink solution in an infinite space

$$P^2 - P_{atm}^2 = \frac{Q_v P^* \mu}{2 \pi k_a (L - l)} \ln \left\{ \frac{z - l + \sqrt{r^2 + (z - l)^2}}{z - L + \sqrt{r^2 + (z - L)^2}} \right\} \quad (2-23)$$

where

l = z -coordinate of the top of the well screen

L = z -coordinate of the bottom of the well screen

The limitation to this analytical solution is that accounting for the effects of atmospheric and impermeable boundaries typically requires the summation of a large number of additional terms. A solution for two-dimensional flow to a well in a vertically bounded aquifer can be found using the method of images presented in Appendix E. The solution is sufficiently complex, however, that there is little advantage to using the analytical form over one of the widely available numerical model tools listed in Appendix C. A graphical method for predicting pressure distribution around an extraction or injection well is provided by Shan and others (1992). The methodology described in this paper is a valuable tool for the system designer.

(12) Travel time is useful in SVE/BV design for determining the required flow rates and well spacings necessary to achieve a desired air exchange rate. Travel time can be obtained by integrating the reciprocal of the seepage velocity along a streamline (path of flow):

$$t = \int \left(\frac{l}{q_s} \right) ds \quad (2-24)$$

where

s = distance along a streamline, and

q_s = seepage velocity

The seepage velocity can be obtained from Darcy's Law:

$$q_s = \frac{k_a}{n_a \mu} \nabla P \quad (2-25)$$

and the gradient of pressure can be obtained from the appropriate steady-state flow equation.

Assuming incompressible flow, the gradient of pressure for one-dimensional radial flow is:

$$\frac{dP}{dr} = \frac{Q_v \mu}{2 \pi b k_a r} \quad (2-26)$$

which can be integrated using Equation 2-24 to obtain:

$$t = \frac{\pi r^2 b n_a}{Q_v} \quad (2-27)$$

Equation 2-27 is equivalent to the pore volume of a cylinder surrounding an extraction well, divided by the discharge of the well.

(a) For the flow of a compressible gas, the integration indicated by Equation 2-24 generally requires numerical techniques. Simple finite-difference algorithms may be used for linear or radial one-dimensional flow, whereas more sophisticated particle tracking routines may be used for two-dimensional or three-dimensional flow. Shan, Falta, and Javandel (1992) provide travel times from the ground surface to an extraction well for various well screen positions in a vadose zone with an upper atmospheric boundary and a lower impermeable boundary. The travel times are provided in dimensionless form, allowing application to a particular field problem through a simple scaling procedure.

(b) King (1968) also provides vertical travel times from an injection well to the ground surface in a vadose zone with an upper atmospheric boundary and a lower impermeable boundary. This represents the minimum travel time from an injection well to the ground surface. The vertical travel times are provided in dimensionless form for a variety of well screen positions.

d. *Transient vapor flow.* The partial differential equation for transient flow is

$$\nabla \cdot (k_a \nabla P) = 2 n_a \mu \frac{\partial P}{\partial t} \quad (2-28)$$

(1) McWhorter (1990) developed an exact solution to a more rigorous form of Equation 2-14 accounting for gas slippage and pressure dependent viscosity. McWhorter's solution applies for one-

dimensional radial flow with upper and lower impermeable boundaries. A simplified case of McWhorter's solution is presented in Appendix D, for analysis of transient air permeability test data.

(2) Johnson, Kemblowski, and Colthart (1990b), following Muscat, (1931), proposed linearizing Equation 2-14 by expressing P^2 as the product of atmospheric pressure P_{atm} and a deviation from that pressure P_p . The resulting equation expressed in one-dimensional radial coordinates is

$$\nabla \bullet (\nabla P') = \frac{n_a \mu}{k_a P_{atm}} \frac{\partial P'}{\partial t} \quad (2-29)$$

(3) Equation 2-29 has the same form as the linearized Boussinesq equation for groundwater flow. This equation essentially treats air as an incompressible fluid.

(4) Massmann (1989) determined that the errors introduced by substituting P for P^2 are negligible for vacuums less than 0.2 atmospheres, gauge. Accordingly, Massmann proposed that groundwater flow models based on the linearized Boussinesq equation can be applied to vapor flow, with the substitution of pressure head (i.e., $P/\rho g$) for hydraulic head, and soil gas conductivity for hydraulic conductivity. Model simulations should be limited to vacuums less than 0.2 atmospheres, gauge, i.e., in accord with the assumption of incompressible flow.

(5) In one-dimensional radial coordinates, Equation 2-29 is:

$$\frac{1}{r} \frac{\partial}{\partial r} \left(r \frac{\partial P'}{\partial r} \right) = \frac{n_a \mu}{k_a P_{atm}} \frac{\partial P'}{\partial t} \quad (2-30)$$

The solution to this equation for a constant sink at $r = 0$, with $P = P_{atm}$ at $r = 4$, is (Johnson et al. 1990b):

$$P - P_{atm} = \frac{Q_v \mu}{4 \pi b k_a} \int_u^\infty \frac{e^{-x}}{x} dx \quad (2-31)$$

where

Q = volumetric flow rate [$L^3 T^{-1}$]

b = the thickness of the vadose zone or stratum of interest [L], and

$$u = \frac{r^2 n_a \mu}{4 k_a P_{atm} t} \quad (2-32)$$

(a) The integral in Equation (2-31) is known as the Theis well function (Theis 1935), where x is a dummy variable of integration. The Theis well function is commonly used for analysis of groundwater pump test data in confined aquifers. Related well functions have also been developed for unconfined radial flow (Neuman 1975) and leaky radial flow (Hantush and Jacob 1955).

(b) The Theis solution is accomplished by combining distance and time into the Boltzmann variable, u . If u is sufficiently small, then the integral in Equation 2-31 can be approximated using the first two terms of a Taylor series expansion. Using this approximation, Equation 2-31 reduces to:

$$P - P_{atm} = \frac{Q_v \mu}{4 \pi b k_a} \left(\ln \frac{4 k_a P_{atm} t}{r^2 n_a \mu} - 0.5772 \right) \quad (2-33)$$

Equation 2-33 is commonly known as the Cooper-Jacob approximation. Note that the pressure drawdown ($P - P_{atm}$) varies linearly with $\ln(t)$. This equation is commonly used for transient air permeability test analysis (Appendix D).

(c) Equations 2-31 through 2-33 are based on the assumption of horizontal radial flow, with upper and lower impermeable boundaries. Beckett and Huntley (1994) suggest that these conditions rarely occur, even where asphalt or concrete surface covers are present. The effect of vertical flow through a leaky surface cover can be simulated by adding a leakage term to the partial differential equation for radial flow:

$$\frac{\partial^2 P}{\partial r^2} + \frac{1}{r} \frac{\partial P}{\partial r} - \frac{L \mu}{k_a \rho g b} = \frac{n_a \mu}{k_a P_{atm}} \frac{\partial P}{\partial t} \quad (2-34)$$

where L is the leakage rate.

(d) For incompressible flow through a surface cover of thickness b_v and vertical air permeability k_v , the leakage rate per unit area is:

$$L = \frac{k_v \rho g}{\mu} \frac{(P - P_{atm})}{b_v} \quad (2-35)$$

Substituting L into Equation 2-34 yields:

$$\frac{\partial^2 P}{\partial r^2} + \frac{1}{r} \frac{\partial P}{\partial r} - \frac{k_v}{k_a} \frac{(P - P_{atm})}{b b_v} = \frac{n_a \mu}{k_a P_{atm}} \frac{\partial P}{\partial t} \quad (2-36)$$

Introducing a *leakage factor* B , defined by:

$$B = \sqrt{\frac{k_a b_v b}{k_v}} \quad (2-37)$$

yields an equation similar to the leaky aquifer equation for groundwater flow (McWhorter and Sunada, 1977):

$$\frac{\partial^2 P}{\partial r^2} + \frac{1}{r} \frac{\partial P}{\partial r} - \frac{P - P_{atm}}{B^2} = \frac{n_a \mu}{k_a P_{atm}} \frac{\partial P}{\partial t} \quad (2-38)$$

(e) Employing the Hantush-Jacob leaky aquifer solution, available in most groundwater hydraulics texts, the solution to this equation is:

$$P - P_{atm} = \frac{Q_v \mu}{4 \pi b k_a} W(u, \frac{r}{B}) \quad (2-39)$$

where $W(u, r/B)$ is the leaky well function. For vapor flow, the Boltzmann variable u is defined in Equation 2-32.

(f) Beckett and Huntley (1994) found a superior fit of field permeability test data using the leaky well function than that using the Theis well function at five sites. They conclude that vertical air leakage is the rule, rather than the exception. They state that use of the Theis well function (Equation 2-31), including its Taylor series approximation (Equation 2-33), results in overestimation of the air permeability and the allowable vapor extraction rate, and underestimation of the time required to achieve site cleanup.

e. The pseudo-steady state. For one-dimensional radial flow, the Cooper-Jacob approximation (Equation 2-33) predicts that the pressure difference between any two radial distances (provided $u \leq 0.01$) is

$$P_2 - P_1 = \frac{Q_v \mu}{4 \pi b k_a} \left(\ln \frac{4 k_a P_{atm} t}{r_1^2 n_a \mu} - \ln \frac{4 k_a P_{atm} t}{r_2^2 n_a \mu} \right) \quad (2-40)$$

for $r_2 > r_1 > 0$ and $(P_2 - P_1) < P_1$

If P_1 and P_2 are measured at the same time, then

$$P_2 - P_1 = \frac{Q_v \mu}{4 \pi b k_a} \left(\ln \frac{r_2}{r_1} \right) \quad (2-41)$$

(1) This is identical to the steady-state equation for radial *incompressible* flow. As pointed out by McWhorter and Sunada (1977), this indicates that although pressure may be changing with time, the time rate of change of P is independent of r (as long as $u \leq 0.01$). That is, while pressure measurements may vary with time, the difference in pressures between any two points remains constant (Figure 2-6).

(2) The foregoing analysis demonstrates that transient test data from multiple observation points can be analyzed using equations for steady-state radial flow, provided that pressure measurements are recorded simultaneously. This type of analysis is referred to as the pseudo-steady state (McWhorter and Sunada 1977). Where applied vacuums or pressures exceed 0.2 atmospheres gauge, pseudo-steady state analyses may be more accurate than Theis or Cooper-Jacob type analyses, since the effects of pressure-dependent density can be accommodated using steady-state solutions.

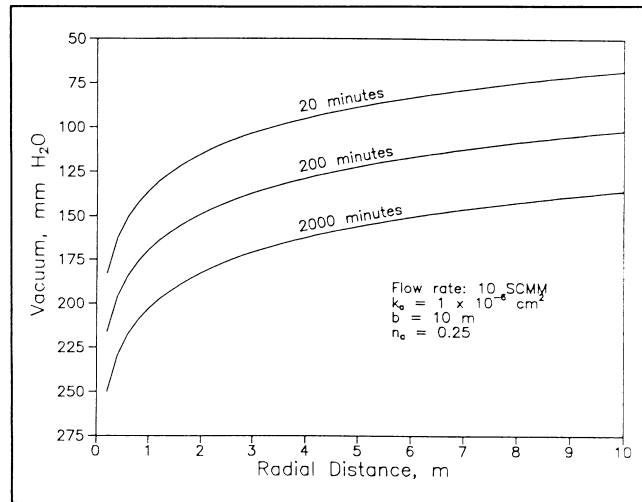


Figure 2-6 Transient pressure distributions calculated using the Cooper-Jacob approximation ($\mu \leq 0.01$)

2-5. Biodegradation Kinetics

a. *Fundamental principles.* Biodegradation can be expressed mathematically as a hyperbolic function, as in Michaelis-Menten kinetics equation:

$$R = - \frac{VC}{K + C} \quad (2-42)$$

with reaction rate R , maximum biodegradation velocity V , and biodegradation half-saturation constant K . The half-saturation constant is the contaminant concentration at which the biodegradation velocity is equal to half of its maximum value. The negative sign on the right-hand side indicates that the contaminant is

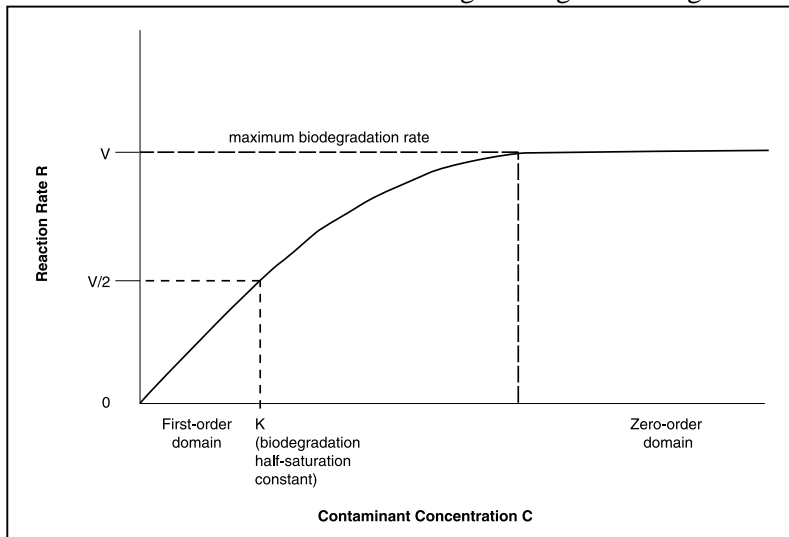


Figure 2-7 Biodegradation Reaction Rate as a Function of Substrate Concentration

being consumed. Reaction rate versus substrate concentration is sketched in Figure 2-7. Oxygen is assumed not to be limiting because abundant oxygen is provided to the unsaturated zone during BV. (This may often be an inappropriate assumption, see para 2-5a(6) below.)

(1) In equation 2-42, at high contaminant concentrations, K drops out and the C 's cancel. Biodegradation velocity is at its maximum, V , and biodegradation is zero order, i.e., the rate is independent of contaminant concentration

$$R = -V \quad (\text{when } K \ll C)$$

(2) At low contaminant concentrations, R reduces to a first-order expression in which the biodegradation rate is equal to a first-order rate constant F ($F = V/K$) times contaminant concentration

$$R = -FC \text{ (when } K \gg C) \quad (2-44)$$

(3) First-order kinetics are often appropriate in BV applications, in which case

$$C_t = C_o \exp(-Ft) \quad (2-45a)$$

$$\ln\left(\frac{C_t}{C_o}\right) = -Ft \quad (2-45b)$$

with initial concentration C_o and concentration at some later time C_t . If the first-order rate constant F is known, the time t required to achieve a treatment goal C_t can be estimated.

(4) The concept of half-life is derived from the latter equation. The half-life is the time required to degrade half of some initial contaminant concentration

$$\ln(0.05) = -Ft_{1/2} \quad (2-46a)$$

$$t_{1/2} = \frac{0.693}{F} \quad (2-46b)$$

(5) The first-order rate constant can be estimated from concentration versus time data, e.g., from microcosm or column studies. For example, if a reaction is first order, a semilog plot of Equation 2-45a gives a straight line whose slope is F . Kinetic parameters and half-lives are, of course, site-specific, depending on such factors as microbial population, moisture content, and availability of nutrients.

(6) It is critical to understand, however, that at many sites, contaminants are located both within the pores through which air flows, *and* in soil pores that only experience gas exchange through diffusive processes. Bacteria that must rely on diffusion to receive oxygen for aerobic biodegradation will have reaction rates that are also dependent on oxygen concentration. In these situations, equation 2-42 is no longer applicable, and the curve depicted in Figure 2-7 will be characteristically different. Indeed, oxygen uptake rates at many sites have been found to be first order with respect to oxygen, suggesting that oxygen diffusion, not contaminant concentration, controls contaminant removal rates. Therefore it is more practical to focus attention on oxygen respiration rather than on contaminant degradation kinetics. Oxygen concentrations are easily and directly measurable in the field, and may be related to contaminant removal through adoption of appropriate stoichiometric assumptions, as presented in paragraph 4-2g(4).

b. Recent applications. Few models of unsaturated zone biodegradation and BV have been developed. Jury et al. (1990) included first-order biodegradation in an analytical model of volatilization losses of subsurface VOC contamination. Corapcioglu and Baehr (1987) and Baehr and Corapcioglu (1987) developed a sophisticated one-dimensional finite difference model of unsteady multiphase multicomponent organic transport with static NAPL and air phases. The model assumed that biodegradation was limited by oxygen -- rather than substrate or nutrient -- availability.

(1) Bentley and Travis (1991) include biodegradation in a three-dimensional finite-difference model capable of simulating gas and liquid flow and multicomponent solute transport under saturated and unsaturated conditions. Michaelis-Menten kinetics are used for biodegradation, and BV situations are simulated.

(2) Ostendorf and Kampbell (1991) present an analytical model of unsaturated zone biodegradation of hydrocarbon vapors under natural (unvented) conditions. Gaseous diffusion is balanced against biodegradation. Oxygen and hydrocarbon vapors are modeled and related stoichiometrically as coupled constituents. Biodegradation is not simplified as zero or first order (Equation 2-28 was used). The model is fit to field probe cluster data (i.e., oxygen and total combustible hydrocarbon concentrations) by optimizing values of V and K .

(3) Ostendorf and Kampbell (1990) present an analytical BV model which balances storage, linear sorption, vertical advection, and Michaelis-Menten kinetics (Equation 2-42). No residual contamination is present in the unsaturated zone modeled. The model is tested against laboratory microcosm and field data. Good agreement endorsed both the simple modeling approach and the use of microcosms to predict field kinetics. The model is also used to simulate remediation times at a BV site.

(4) The Ostendorf and Kampbell (1990) paper also derives a microcosm model, which is an unsteady balance of linear adsorption, influx from the microcosm headspace, and Michaelis-Menten biodegradation. Fitting microcosm concentration versus time data to the model yields estimates of V and K , which in turn can be used in BV models. This microcosm model is also used in Richards, Ostendorf, and Switzenbaum (1992).

(5) Moyer (1993) presents an analytical model for column studies of BV, in which kinetic parameters are determined by modeling vertical profiles of hydrocarbon vapor concentration. These are compared with biodegradation kinetics for the same location at the same site determined from probe cluster data (Ostendorf and Kampbell 1991) and laboratory microcosms (Richards, Ostendorf, and Switzenbaum 1992). Agreement is good even though different models were used, and different concentrations and time and length scales were involved.

2-6. Use of Models in SVE/BV Strategy

Computer modeling is an important tool that can contribute significantly to all phases of an SVE/BV project. Readily available models are summarized in Appendix C. Use of models throughout an SVE/BV project is described below.

a. Technology screening. The technical feasibility of SVE/BV is typically related to required expenditures. The following question is often asked, "What would be the order-of-magnitude installation costs of an SVE/BV system?" Installation costs are controlled by the number of extraction points, the

physical spacing of extraction points, the sizing/numbers of blowers required to extract vapors, and the type/size of offgas treatment equipment. Models can be used to quickly provide order-of-magnitude estimates of the total required airflow and the spacing of extraction points so that preliminary estimates of installation costs can be obtained. This preliminary modeling should not be substituted for pilot testing and detailed design. Typically, the effort includes modeling of a broad range of permeabilities, porosities, gas constants, gas molar masses, and viscosities to obtain maximum and minimum estimates of vapor production rates and numbers of extraction points. Contact between the modelers and the site characterization team is strongly encouraged. Screening models typically require no more than one or two days of labor by the project engineer. Significantly more effort is usually not appropriate if investigations have been limited and pilot testing has not been performed.

(1) Screening vapor transport models such as HyperVentilate and VENTING are typically used during the technology screening portion of a project to provide order-of-magnitude estimates of the time which would be required to remediate if SVE/BV was used. The programs can be used by most project engineers and simulations provide easy to understand output (e.g., mass of benzene extracted versus time). However, these models usually include at least one lumped parameter (e.g., removal efficiency) which accounts for the net effect of several factors. These lumped parameters have little physical meaning and the assumed value can significantly change the predicted vapor concentrations and remediation times. Therefore, novice modelers should always ensure that their work receives peer review from more experienced practitioners.

(2) A question which is often asked is, "What would be the O&M costs associated with the system and how long would the system be expected to operate (order-of-magnitude estimate)?" Simulations are performed assuming a range of plausible input parameters to estimate the concentrations of contaminants in offgas (so that treatment costs can be estimated) and to estimate the range of time which might be required to achieve remedial objectives (so that total O&M costs can be estimated). For example, screening simulations may be used to estimate that a hypothetical SVE/BV system for a moderately volatile compound would have an O&M cost of between \$20,000 and \$40,000 per year and may be expected to operate between 2 and 4 years. Therefore, O&M expenditures (not including installation costs or inflation) might range from \$40,000 to \$160,000. A parallel analysis might reveal that excavation with onsite bioremediation would cost \$70,000 to \$90,000 over a one-year period. In this scenario, it might be concluded that the short-term time frame and smaller potential cost range associated with the second remedial option would be preferred.

(3) Detailed vapor transport models are most often used to aid in the optimization of large SVE/BV systems with complicated contaminant distributions. Detailed vapor transport models are not usually used for small SVE/BV systems (e.g., less than five extraction points). In those scenarios, project engineers typically rely on empirical trends from pilot tests or from operation of the full-scale system to estimate times for completion of remediation.

(4) The construction of detailed vapor transport models almost always requires the input of several parameters that have not been measured (e.g., dispersion coefficients or partitioning coefficients). In addition, the calibration process often requires adjustment of parameters to achieve a fit between actual and simulated data. That process is very time consuming and requires considerable judgment based on experience. Consequently, experienced modelers should be used if detailed vapor transport modeling will be performed.

b. Pilot test design. When the decision has been made to pilot test an SVE/BV system, simple simulations are sometimes performed to aid in design of the pilot test. These simulations are typically

performed to estimate the range of vapor flow rates which might be expected from one extraction point so that the appropriate equipment is mobilized, and to estimate the potential discharge concentrations to select appropriate emissions treatment for the pilot test. In addition, simulations are frequently used to estimate the maximum and minimum potential radii of influence of the pilot extraction point so that observation points for measuring soil vapor pressures are located appropriately. These simple simulation efforts are typically performed in about one day.

c. Extrapolation of pilot test data for full-scale design. After pilot testing has been completed, the preliminary model is typically updated by calibrating the model to pilot test data.

(1) Perhaps the most useful application of pilot test data for design of full-scale systems is for determination of pressure and vacuum requirements. When the design flow rate has been selected, the pressure or vacuum required to achieve the design flow rate must be determined. Although vacuum at the well screen can be calculated using Equations 2-20 or 2-27, wellbore vacuums generally exceed these values due to well inefficiency. Unfortunately, well inefficiencies are difficult to predict, as they appear to be controlled by capillary pressure-saturation relations. Results of pilot test data, however, provide a direct measurement of the pressure or vacuum necessary to develop a particular flow rate. A plot of flow vs. vacuum obtained from stepped rate pumping tests can be used to determine pressure or vacuum requirements at the design flow rate. In conjunction with data regarding friction losses through piping and equipment, these data are used for equipment sizing and determination of system power requirements.

(2) The process includes incorporation of measured vapor parameters and permeability estimates followed by specification of the pilot extraction point location and vapor extraction rate which was used during the pilot test. The model is then run and simulated vapor pressure distributions are compared to actual measured vapor pressure distributions. The simulated pressure distributions will be different from actual distributions after the first run. This is usually due to soil permeability variations and unexpected boundary conditions (e.g., utility conduits). Because of this, calibration becomes an iterative process of slightly changing assumed soil properties and/or boundary conditions in certain areas followed by repeated runs until simulated pressure distributions are within an acceptable range of the measured distributions. The acceptable range is usually defined by the amount of error associated with the pilot test measurements.

(3) Once a model has been calibrated to pilot test data, the model can be used to simulate varied numbers, locations, and flow rates from/to extraction points and air injection points (see Figure 5-11). When a simulated scenario fulfills design criteria (e.g., sufficient contaminant removal within an acceptable time frame), the flow rates from extraction points are tabulated for specification of equipment and appropriate monitoring locations are chosen. The simulation process also includes a sensitivity analysis in which parameters (e.g., vapor temperature) are varied within a plausible range to determine the potential effect on predicted flow rates and pressure distributions. These sensitivity runs are used to ensure that specified equipment will be capable of handling the full range of potential pressures and flows.

d. System operation. Many large SVE/BV systems are anticipated to operate for several years. Modeling can help optimize operation of longer duration systems.

(1) All contaminated areas in these large systems will not be remediated at the same rate due to variations in soil conditions and contaminant concentrations. Consequently, certain portions of the system may be turned off earlier than other portions. Conversely, operational data may indicate the need to add vapor extraction or injection points in other areas. Models are sometimes calibrated to the operational data

to allow the effects of turning off components to be predicted (often to fulfill a regulatory obligation) or to optimize the locations of potential system expansions.

(2) When portions of SVE/BV systems are turned off earlier than other portions, there is frequently a concern that contaminants may migrate back into areas which have been turned off, that contaminants may partition into the vapor phase from the sorbed phase, or that contaminants may slowly partition into the vapor phase from underlying groundwater which has not been fully remediated. Simulations may be performed to estimate if contaminant concentrations might “rebound” in areas where systems are turned off and to determine which operational changes would be required to prevent concentration “rebound.” Appendix F presents a methodology for performing rebound assessments and the mathematical framework for interpreting rebound data.